THE JOURNAL OF BIOLOGICAL CHEMISTRY VOL. 288, NO. 16, pp. 11038–11046, April 19, 2013

Chitoporin from *Vibrio harveyi*, a Channel with Exceptional Sugar Specificity

Received for publication, January 17, 2013, and in revised form, February 26, 2013 Published, JBC Papers in Press, February 27, 2013, DOI 10.1074/jbc.M113.454108

Wipa Suginta[‡1], **Watcharin Chumjan**[‡2], **Kozhinjampara R. Mahendran**[§], **Albert Schulte**[‡], **and Mathias Winterhalter**[§3]

From the [‡]*Biochemistry-Electrochemistry Research Unit, Schools of Chemistry and Biochemistry, Institute of Science, Suranaree University of Technology, Nakhon Ratchasima 30000, Thailand and the* [§]*School of Engineering and Science, Jacobs University Bremen, 28759 Bremen, Germany*

Background: *Vibrio harveyi* chitoporin (*Vh*ChiP) was recently identified as a pore-forming channel responsible for chitooligosaccharide uptake through the outer membrane of *V. harveyi*.
Results: Kinetic analysis revealed that *Vh*ChiP was several orders of magnitude more active than other known sugar-specific porins.
Conclusion: *Vh*ChiP is a channel with exceptional sugar specificity.
Significance: The high activity of *Vh*ChiP reflects an evolutionary adaptation required for *V. harveyi* to thrive under extreme aquatic conditions.

Chitoporin (*Vh*ChiP) is a sugar-specific channel responsible for the transport of chitooligosaccharides through the outer membrane of the marine bacterium *Vibrio harveyi*. Single channel reconstitution into black lipid membrane allowed single chitosugar binding events in the channel to be resolved. *Vh*ChiP has an exceptionally high substrate affinity, with a binding constant of $K = 5.0 \times 10^6$ M^{-1} for its best substrate (chitohexaose). The on-rates of chitosugars depend on applied voltages, as well as the side of the sugar addition, clearly indicating the inherent asymmetry of the *Vh*ChiP lumen. The binding affinity of *Vh*ChiP for chitohexaose is 1–5 orders of magnitude larger than that of other known sugar-specific porins for their preferred substrates. Thus, *Vh*ChiP is the most potent sugar-specific channel reported to date, with its high efficiency presumably reflecting the need for the bacterium to take up chitin-containing nutrients promptly under turbulent aquatic conditions to exploit them efficiently as its sole source of energy.

Vibrio harveyi is a Gram-negative, bioluminescent, marine bacterium of the family Vibrionaceae. It is found free-living in tropical marine waters and also commensally as a component of the gut microflora of marine animals. The bacterium is both a primary and an opportunistic pathogen of marine animals, triggering a lethal disease called luminous vibriosis (1), which affects marine fish and prawn-farming operations worldwide (2, 3). *V. harveyi* is a fast growing bacterium under both aerobic and anaerobic conditions. Accordingly, it can cause the "milky seas" effect, in which a uniform blue glow is emitted from the seawater and which is apparent during the night. Sometimes the glow covers nearly 16,000 km^2.

In marine ecosystems, chitin-containing substances are major sources of carbon and nitrogen for marine vibrios. The catabolic cascade of chitin utilization has been proposed to be a complex system, involving a large number of genes that are orchestrated under the stringent control of the chitin-induced operon (4). In brief, the multistep chitin degradation pathway involves (i) chitin sensing and degradation; (ii) chitooligosaccharide uptake into the periplasm; (iii) degradation of the transported products to GlcNAc and $GlcNAc_2$, which are then transported farther into the cytoplasm; and (iv) conversion of GlcNAc intermediates to Fru-6-P and NH_3^+, which are metabolized for energy production and biosynthesis (5–7).

Chitoporin was initially identified in the marine bacterium *Vibrio furnissii* as part of the chitin catabolic cascade. Its function was partially revealed by gene knockdown and $GlcNAc_2$ uptake assays (8). Later, the gene encoding chitoporin was also identified in the genome of other marine bacteria, such as *Vibrio cholera* and *Shewanella* spp. (6, 9, 10). However, the specific function of chitoporin as a sugar-specific channel had never been clearly elucidated. We recently employed black lipid membrane (BLM)[4] reconstitution and liposome swelling assays to demonstrate that chitoporin from *V. harveyi* (*Vh*ChiP) is a pore-forming channel that performs highly specific translocation of chitooligosaccharides (11). In the present study, we focused on the kinetic evaluation of single chitooligosaccharide translocation through a single *Vh*ChiP. Detailed assessment of the kinetic parameters suggested that *Vh*ChiP acts as a highly specific channel, interacting with chitooligosaccharides, especially chitohexaose, down to nanomolar concentrations.

EXPERIMENTAL PROCEDURES

Vectors and Bacterial Strains—A cDNA fragment of 1.1 kilobase pairs corresponding to the full-length *Vh*ChiP gene was

[1] Humboldt Fellow supported by an Alexander von Humboldt Fellowship for Experienced Researchers from the Alexander von Humboldt Foundation (Bonn, Germany). To whom correspondence should be addressed: Suranaree University of Technology, 111 University Ave., Nakhon Ratchasima 30000, Thailand. Fax: 66-44-226-187; E-mail: wipa@sut.ac.th.
[2] Supported by CHE-PhD-SW Scholarship Contract 60/2550 from the Commission of Higher Education, Ministry of University Affairs (Bangkok, Thailand).
[3] Supported by Deutsche Forschungsgemeinschaft (DFG) Grant WI 2278/18-1.

[4] The abbreviations used are: BLM, black lipid membrane; *Vh*ChiP, *V. harveyi* chitoporin.

cloned into the Novagen expression vector pET-23d(+) (Merck). *Escherichia coli* host strain BL21(DE3) Omp8 Rosetta was a kind gift from Professor Dr. Roland Benz (Jacobs University Bremen, Bremen, Germany). This *E. coli* strain was genetically engineered to carry defective genes encoding the major outer membrane porins OmpA, OmpC, OmpF, and LamB, making it suitable for production of an exogenous porin (12).

Recombinant Expression and Protein Purification—The *E. coli* BL21(DE3) Omp8 Rosetta host strain was transformed with plasmid pET-23d(+)/*Vh*ChiP. Expression and preparation of recombinant *Vh*ChiP were performed following the protocols described by Garavito and Rosenbusch (13) and Rosenbusch (14). In brief, transformed cells were grown at 37 °C in LB liquid medium containing 100 μg/ml ampicillin and 25 μg/ml kanamycin. At A_{600} = 0.5–0.7, isopropyl β-D-thiogalactopyranoside was added to a final concentration of 0.5 mM. Cell growth was continued for an additional 6 h, and cells were then harvested by centrifugation at 4500 × *g* for 20 min at 4 °C. The cell pellet was resuspended in buffer containing 20 mM Tris-HCl (pH 8.0), 2.5 mM $MgCl_2$, 0.1 mM $CaCl_2$, 10 μg/ml DNase I, and 10 μg/ml RNase A. Cells were lysed by sonication on ice for 10 min (30% duty cycle, amplitude setting of 20%) using a SONOPULS ultrasonic homogenizer with a 6-mm diameter probe. Recombinant *Vh*ChiP was extracted from the peptidoglycan layer with SDS based on the method of Lugtenberg and Van Alphen (15). Briefly, SDS was added to the cell suspension to a final concentration of 2% (w/v), and incubation was carried out for 1 h at 60 °C with gentle shaking. The crude extract was then centrifuged at 40,000 × *g* for 60 min at 4 °C. The pellet, which at this stage included the cell envelopes, was resuspended in 20 mM phosphate buffer (pH 7.4) containing 0.125% (v/v) *n*-octylpolyoxyethylene (Alexis Biochemicals, Lausanne, Switzerland) using a Potter-Elvehjem homogenizer. The suspension was incubated at 37 °C with gentle shaking for 1 h and then centrifuged at 100,000 × *g* for 40 min at 4 °C. The new pellet, now rich in outer membranes, was resuspended in 20 mM phosphate buffer (pH 7.4) containing 3% (v/v) *n*-octylpolyoxyethylene, and the suspension was incubated at 37 °C for 60 min. Insoluble material was removed by centrifugation at 100,000 × *g* for 40 min at 20 °C. After exchange of the detergent with 0.2% (v/v) lauryldimethylamine oxide (Sigma-Aldrich) by dialysis, the *Vh*ChiP-rich sample was subjected to ion exchange chromatography using a HiTrap Q HP prepacked column (5 × 1 ml) connected to an ÄKTAprime Plus FPLC system (GE Healthcare). Bound proteins were eluted with a linear gradient of 0–1 M KCl in phosphate buffer containing 0.2% (v/v) lauryldimethylamine oxide. The purity of the eluted proteins was confirmed by SDS-PAGE. Fractions containing only *Vh*ChiP were pooled, and the protein concentration was determined using the Pierce BCA protein assay kit (Bio-Active Co., Ltd., Bangkok, Thailand).

BLM Measurements and Single Channel Analysis—BLM measurements and single channel analysis were performed following the methods described previously (16–23). Briefly, the lipid bilayer cuvette consisted of two chambers separated by a 25-μm-thick Teflon film. The latter had a small aperture of 60–100 μm in diameter, across which a virtually solvent-free planar lipid bilayer was formed. The chambers were filled with electrolyte solution and Ag/AgCl electrodes (World Precision Instruments, Sarasota, FL) immersed on either side of the Teflon film. The electrolyte solution used was 1 M KCl buffered with 20 mM HEPES (adjusted to pH 7.5). 1,2-Diphytanoyl-*sn*-glycero-3-phosphatidylcholine (Avanti Polar Lipids, Alabaster, AL) was used for lipid bilayer formation. To form the bilayer, the aperture was first pre-painted with 1 μl of 1% (v/v) hexadecane in pentane (Sigma-Aldrich). One of the electrodes (*cis*) was used as the ground electrode, whereas the other (*trans*) was connected to the headstage of an Axopatch 200B amplifier (Axon Instruments, Foster City, CA). The trimeric *Vh*ChiP channel (50–100 ng/ml) was always added to the *cis* side of the lipid membrane. At applied transmembrane potentials of +200 and −200 mV, a single channel was frequently inserted within a few minutes. The protein solution in the chamber was gently diluted by sequential additions of the working electrolyte to prevent multiple insertions. To investigate sugar translocation, chitooligosaccharides of various lengths (chitotriose ($GlcNAc_3$), chitotetraose ($GlcNAc_4$), chitopentaose ($GlcNAc_5$), or chitohexaose ($GlcNAc_6$)) were titrated on the *cis* side or, in separate experiments, on the *trans* side of the membrane. In some experiments, the sugar was titrated on one side and finally diluted, followed by titration on the opposite side. These experiments were tedious, but yielded consistent results.

A fully open channel of the *Vh*ChiP trimer was titrated with discrete concentrations of chitosugar until saturated, typically from nanomolar to micromolar concentrations, although the suitable range of sugar concentrations depended upon which sugar was being studied. Occlusions of ion flow observed as a result of sugar diffusion through the inserted channel were usually recorded for 120 s at transmembrane potentials of +50, −50, +100, and −100 mV. Single channel current measurements were performed with an Axopatch 200B amplifier in the voltage clamp mode, with the internal filter set at 10 kHz. Amplitude, probability, and single channel analyses were performed using pCLAMP version 10.0 software (Molecular Devices, Sunnyvale, CA).

Estimation of Binding Constants—The equilibrium binding constant (K, M^{-1}) was estimated from the reduction of the ion conductance in the presence of increasing concentrations of sugar using Equation 1 (24, 25),

$$\frac{G_{max} - G_{[c]}}{G_{max}} = \frac{I_0 - I_{[c]}}{I_0} = K \cdot c/(1 + K \cdot c) \qquad \text{(Eq. 1)}$$

where G_{max} is the average conductance of the fully open *Vh*ChiP channel, $G_{[c]}$ is the average conductance at a given concentration of a chitosugar ($[c]$), I_0 is the initial current through the fully open channel in the absence of sugar, and $I_{[c]}$ is the current at a particular sugar concentration. The quality of the data is readily seen by inverting Equation 1 into a so-called Lineweaver-Burk plot $(((G_{max} - G_{[c]})/G_{max})^{-1}$ *versus* $([c]^{-1}))$. Single channel analysis was performed to calculate the rates of association and dissociation. The off-rate (k_{off}, s^{-1}) was obtained from Kullman *et al.* (19) (Equation 2),

$$k_{off} = 1/\tau_c \qquad \text{(Eq. 2)}$$

where τ_c is the average residence (dwell) time (s^{-1}) of the sugar molecule in the channel. The on-rate (k_{on}, $M^{-1} \cdot s^{-1}$) is given by $k_{on} = K \cdot k_{off}$.

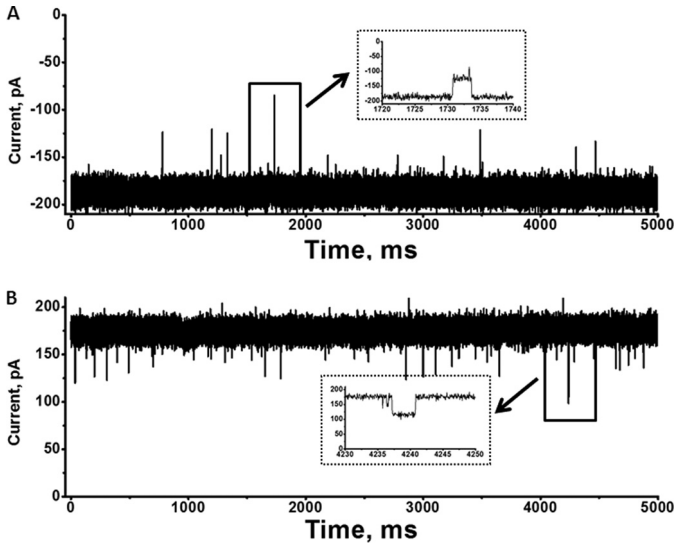

FIGURE 1. **Single trimeric channel recordings of chitoporin in artificial lipid membranes.** The BLM measurements were carried out in electrolyte solution containing 1 M KCl in 20 mM HEPES (pH 7.5). Purified *Vh*ChiP was added on the *cis* side of the chamber. Shown are typical ion current traces of a single *Vh*ChiP channel in the fully open state at applied potentials of +100 mV (*A*) and −100 mV (*B*). The ion currents were normally recorded for a period of 120 s, but representative traces of 5000-ms duration are presented. *Insets*, recordings with an expanded time scale of transient gating at +100 and −100 mV.

RESULTS

Single Channel Properties—As described under "Experimental Procedures," purified *Vh*ChiP was incorporated into solvent-free lipid bilayers, and single channel conductance was estimated to be 1.8 ± 0.13 nanosiemens ($n = 50$). Fig. 1 (*A* and *B*) presents representative current recordings showing current amplitudes of around ±180 pA over 5 s. At applied voltages of +100 and −100 mV, the trimeric channels were fully open, with occasional transient gating (Fig. 1, *insets*). It is important to note that, under the given condition, the pre-inserted membranes were found to be stable, with some lasting beyond 7 h, making them suitable for the kinetic assessment of chitooligosaccharide translocation through the *Vh*ChiP pore.

Channel Specificity—Chitooligosaccharides of various sizes were added on either side of the chamber, and their ability to block ion current was quantified. Fig. 2 shows 100-ms-long recordings of chitooligosaccharide-induced current fluctuations at −100 mV. No blockage was visible when chitobiose was varied up to 400 μM on either the *cis* or *trans* side or when the channel was exposed to maltodextrins (maltopentaose and maltohexaose) or raffinose (data not shown). In marked contrast, after the addition of 5 μM chitosugars, we observed ion current blockages, which depended on the size of the sugar and the side of sugar addition. The ionic current blockages were observed at much greater frequency when the sugar was added on the *cis* side (Fig. 2, *A–D*) compared with the *trans* side (Fig. 2, *E–H*). For instance, current blockage by chitotriose was rarely visible with addition on the *trans* side, whereas significant blocking events were detected when same concentration of chitotriose was added on the *cis* side.

Starting with the *cis* side addition, chitotriose was found to partially interrupt the flow of ions, visible by statistical transient reduction of the channel conductance by one-third (Fig. 2). Chitotriose (Fig. 2*A*), chitotetraose (Fig. 2*B*), and chitopentaose (Fig. 2*C*) blocked one monomer of the single trimeric channel, whereas increasing the sugar length to hexamer (Fig. 2*D*) resulted in the double and triple blocking of the single trimeric channel. Furthermore, chitohexaose exhibited the longest residence time, during which each sugar molecule remained entrapped before leaving the pore. This was clear from single channel analysis, which yielded an average residence time of 6.0 ± 0.7 ms for the chitohexamer. This value decreased rapidly as the number of GlcNAc units in the polymer decreased from five (2.4 ± 0.24 ms) to four (0.33 ± 0.08 ms) and three (0.11 ± 0.05 ms).

Effects of Applied Voltages on Sugar Translocation—We further investigated the effect of applied voltages on sugar translocation from both the *cis* and *trans* sides at various concentrations. As shown in Fig. 3, channel blockage by chitohexaose occurred to a much greater extent for *cis* side addition compared with *trans* side addition. Considering *cis* side addition, the number of blocking events was obviously higher at −100 mV (Fig. 3, *E–H*) than at +100 mV (Fig. 3, *A–D*). This result was reversed with *trans* side addition (data not shown). In both cases, the frequency of blocking events increased with concentration. Fig. 3 (*E–H*) shows that at −100 mV/*cis*, chitohexaose at 0.25 μM blocked only one subunit on average. Two subunits were blocked when the concentration was increased to 1.25 μM, and finally, all three subunits were blocked at 2.5 μM. Similar observations were made with +100 mV/*cis* (Fig. 3, *A–D*), although the frequency of blocking events was much lower.

Fig. 4 presents a detailed analysis of the original traces shown partially in Fig. 3. Plots of the number of blockade events/s (reflecting translocation rate) over a selected range of chitohexaose concentrations were examined for *cis* and *trans* side additions at +100 and −100 mV. The on-rates for chitohexaose moving through open pores decreased as follows: −100 mV/*cis* > +100 mV/*cis* > +100 mV/*trans* ≫ −100 mV/*trans* (Fig. 4*A*). The rates *versus* sugar concentrations from *cis*-to-*trans* yielded saturable curves, but the rates for *trans*-to-*cis* translocation did not reach saturation over the same concentration range.

Applied potentials also affected both τ_o, the time that the monomeric protein channel remains open, and τ_c, the time that the sugar resides within the monomer. As shown in Fig. 4 (*B* and *C*), each setting condition yielded different values of τ_o and τ_c. Nonetheless, all conditions showed a linear decay of τ_o in a concentration-dependent manner, but τ_c does not depend on the concentration.

Rate of Sugar Penetration and Binding Affinity—The characteristic substrate-specific channel activity of *Vh*ChiP was confirmed by enhancement of the on-rate of chitohexaose, relative to that of other oligosaccharides, and by its concentration dependence. As the concentration was increased above 0.1 μM, the on-rate, reflected in the frequency of current blockages, increased, eventually reaching a plateau (Fig. 4*A*). Chitohexaose blocked the ion flow very efficiently even at nanomolar concentrations. A conductance histogram (Fig. 5*A*) shows a continuous increase in the level of monomeric blockage as the channel was titrated with chitohexaose from 0.125 up to 2.5 μM. It is

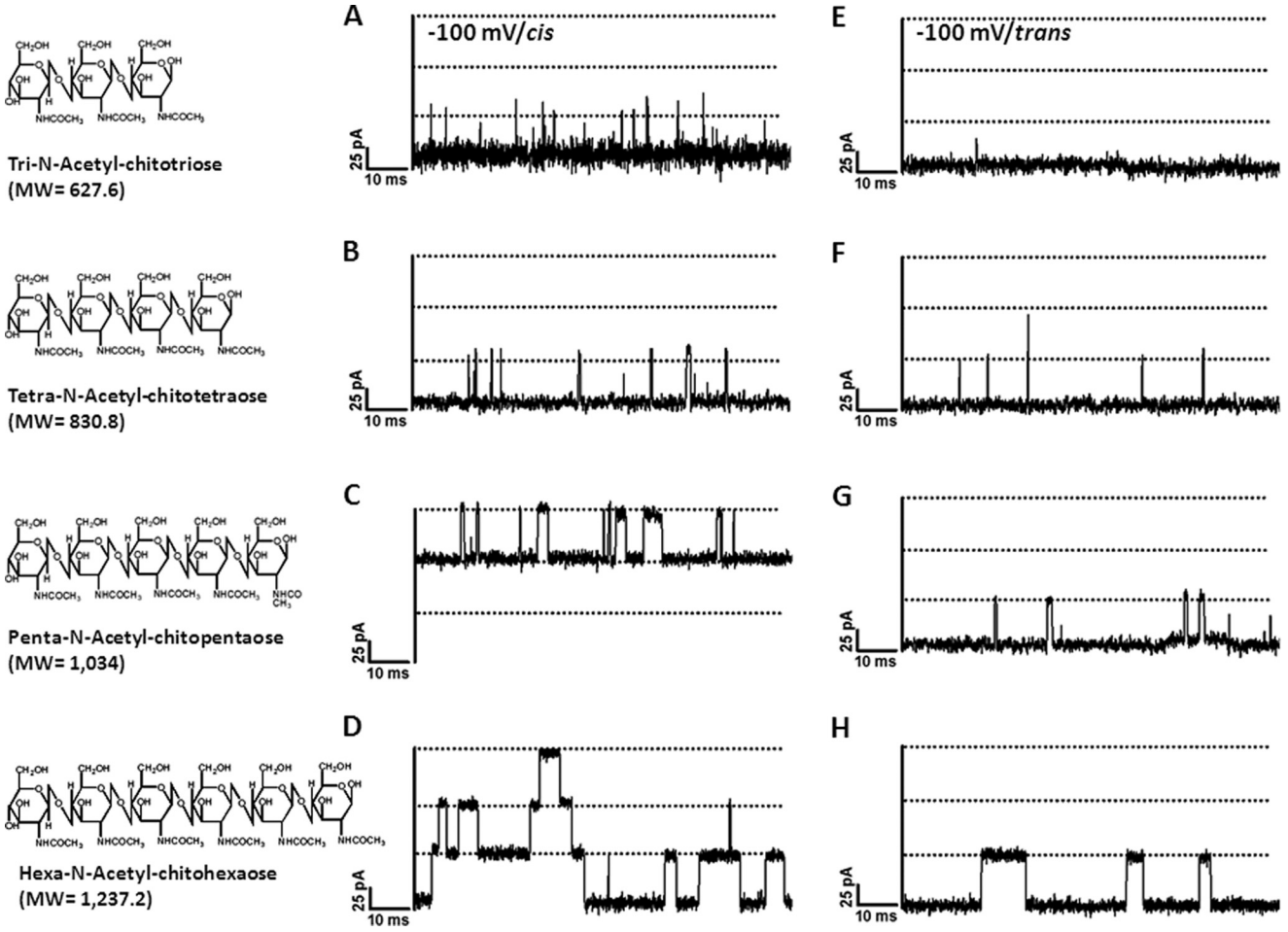

FIGURE 2. **Effect on ion currents of chitooligosaccharide diffusion into chitoporin.** A single trimeric channel of *Vh*ChiP was inserted in an artificial membrane in a fully open state. Chitooligosaccharides of various sizes were then added to a final concentration of 5 μM on either the *cis* side (*A–D*) or *trans* side (*E–H*) of the chamber. *A* and *E*, chitotriose; *B* and *F*, chitotetraose; *C* and *G*, chitopentaose; *D* and *H*, chitohexaose. Ion current fluctuations were monitored for 120 s at applied potentials of +100 and −100 mV. Here, only ion traces for a potential of −100 mV are presented.

shown that the amplitude of the monomeric conductance at 2.5 μM was not much greater than at the previous concentration. Fig. 5*B* displays the related power density spectra. The amplitudes of sugar-induced noise levels were elevated in proportion to the concentration of chitohexaose and correlated well with the levels of monomeric blockage shown in Fig. 5*A*.

Further quantitative analysis of the binding constants was carried out to access the channel affinity. Fig. 6 shows the binding curves of various chitosugars at +100 mV/*cis*. Fitting the curves using a nonlinear regression function derived from Equation 1 yielded typical Michaelis-Menten plots (26). The plot for chitohexaose is hyperbolic, as described above, and saturation was reached within 5 μM (Fig. 6, *inset*). On the other hand, the binding curves of chitotriose, chitotetraose, and chitopentaose did not approach saturation even at 40 μM. Transformation of these binding curves yielded linear double reciprocal plots (Lineweaver-Burk plots) as shown in Fig. 7. Fig. 7*A* shows the Lineweaver-Burk plots for chitotriose, chitotetraose, and chitopentaose at +100 mV/*cis*, whereas Fig. 7*B* shows the Lineweaver-Burk plots for chitohexaose at +100 mV/*cis* compared with −100 mV/*cis*. These Lineweaver-Burk plots allowed the binding constants (K) to be determined as shown in Table 1. As shown in Table 1, the binding constant of chitohexaose was found to be larger than those of other chitosugars at both +100 and −100 mV. The value of K decreased by several orders of magnitude as the polymer length decreased from $GlcNAc_6$ to $GlcNAc_5$ and $GlcNAc_4$. Clearly, the greater binding affinity of the *Vh*ChiP channel for chitohexaose was under the −100 mV/*cis* condition ($K = (5.0 \pm 0.068) \times 10^6\ M^{-1}$). These kinetic data consistently show chitohexaose to be the best substrate for the *Vh*ChiP channel.

DISCUSSION

Marine vibrios require uptake of chitin breakdown products for survival under the critical condition of there being no alternative source of carbon and nitrogen. The chitin catabolic cascade of these bacteria is therefore expected to function efficiently. Once chitin-containing nutrients are detected by the bacteria, a series of events brings the chitinous materials into the cells and metabolizes them as an energy source. Chitin is initially broken down by secreted chitinases (27–29). During chitin degradation, the resulting products are therefore locally enriched in the vicinity of the cells, ready to be rapidly transported through the bacterial outer membrane. Small chitin units (GlcNAc and $GlcNAc_2$) are thought to pass through a general diffusion porin, but permeation of larger chitin oligo-

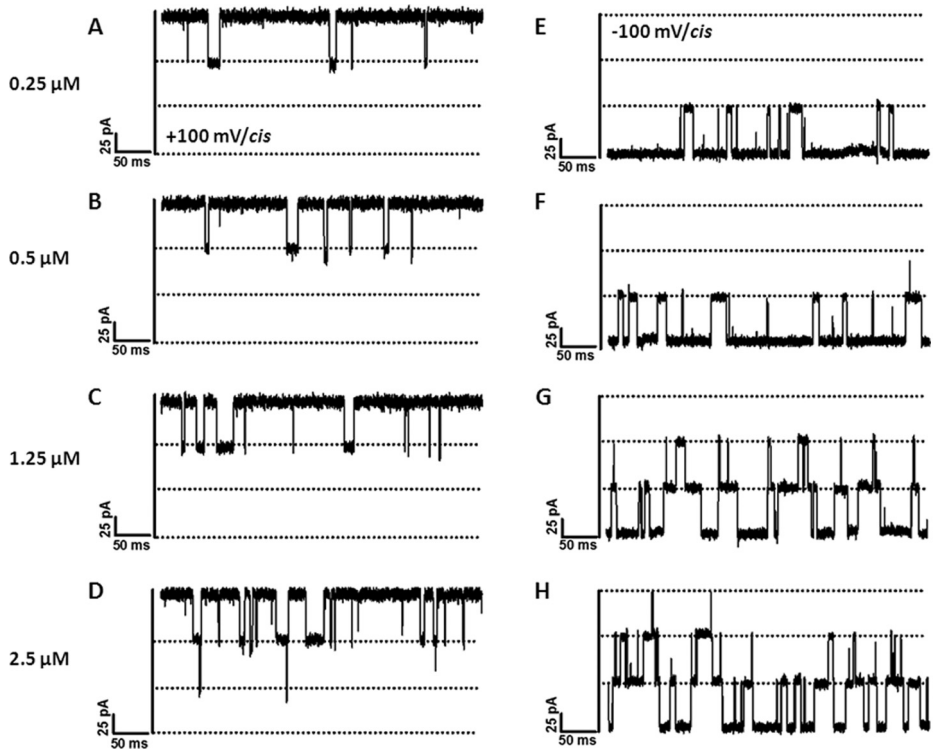

FIGURE 3. **Effects of transmembrane potentials and sugar concentrations on ion currents.** The fully open *Vh*ChiP trimeric channel was exposed to different concentrations of chitohexaose. Ion current blockages at +100 mV (*A–D*) and −100 mV (*E–H*) are shown. Here, we show the titration on the *cis* side.

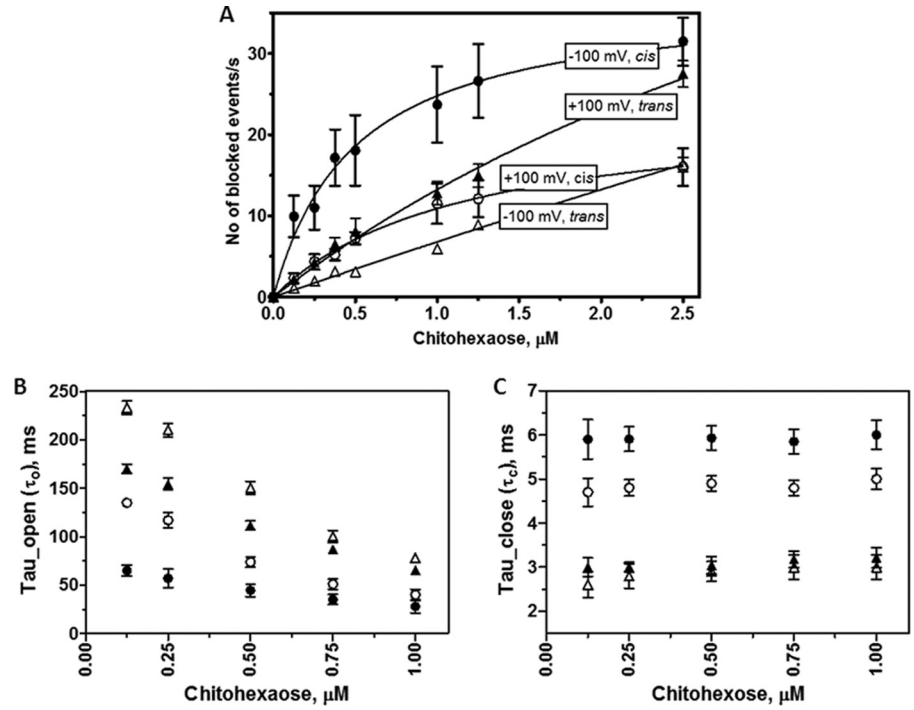

FIGURE 4. **Analysis of ion current blockades at various transmembrane potentials and chitohexaose concentrations.** *A*, plot of the number of binding events *versus* sugar concentrations, comparing +100 and −100 mV and *cis*/*trans* side potential application. *B*, plot of open times (τ_o) *versus* sugar concentrations. *C*, plot of residence times (τ_c) *versus* sugar concentrations. ●, −100 mV/*cis*; ○, +100 mV/*cis*; ▲, +100 mV/*trans*; △, −100 mV/*trans*.

saccharides is facilitated by specific channels, namely chitoporin (8, 30).

To resolve the uncertainty surrounding the function of chitoporin, we previously performed liposome swelling assays to demonstrate possible translocation of chitohexaose, but not other non-chitooligosaccharides, through *Vh*ChiP (11). To quantify translocation, we employed the BLM reconstitution technique based on channel occlusion for ion current. When a *Vh*ChiP channel in the artificially formed membrane was exposed to various types of sugars, the channel responded only

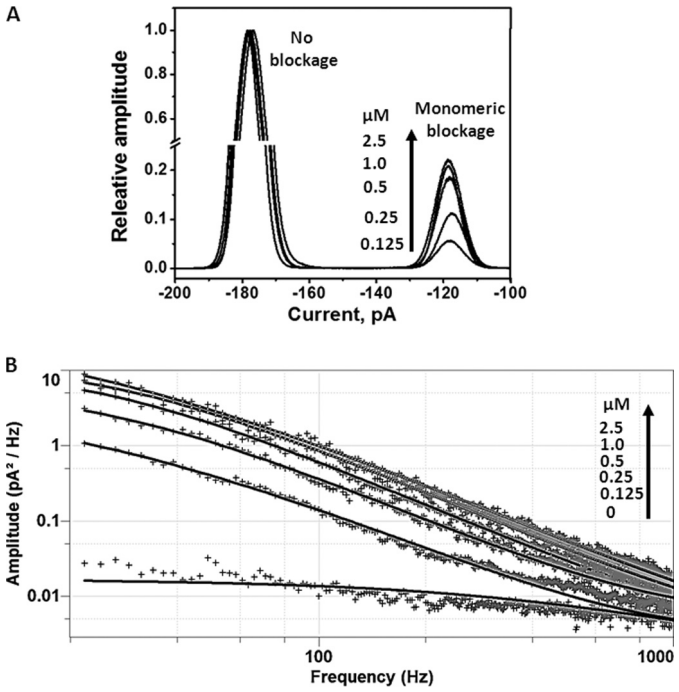

FIGURE 5. **Concentration dependence of channel blockages.** *A*, conductance histogram showing increased frequencies of monomeric blockages as chitohexaose concentrations are increased. The monomeric blockages became steady when the sugar concentrations were above 1 μM. *B*, power density spectra showing the effects of increasing concentrations of chitohexaose on current noise levels. The spectra were fitted without control (the noise level at 0 M sugar) subtraction using the Lorentzian power 2 function available in Clampfit version 10.

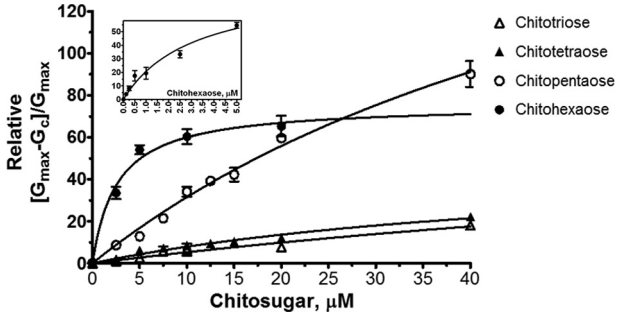

FIGURE 6. **Binding of chitohexaose to *Vh*ChiP compared with that of chitopentaose, chitotetraose, and chitotriose.** The Michaelis-Menten plots were evaluated from the data acquired on the *cis* side at +100 mV. The values are averaged from the BLM data obtained in triplicate. The plots of $(G_{max} - G_{[c]})/G_{max}$ *versus* sugar concentrations (micromolar) were derived from Equation 1. The *inset* shows the plot for chitohexaose at initial concentrations of 0–5 μM.

to chitooligosaccharides, with the degree of responsiveness increasing with greater chain length. The channel was most active with chitohexaose, suggesting some channel specificity for this particular molecule. This observation was analogous to maltoporin-binding maltooligosaccharides, the most effective ligand for this channel being maltoheptaose (31, 32). Note that analysis of the sugar-induced blockages provides information on the presence of sugar in the channel with a residence time limit of 100 μs of events/s. Faster events are not resolvable by this technique.

Regardless of the chain length, the probability of ion current blockade was greater with elevated concentrations of the chitosugars. Fig. 8 represents selected current time traces showing

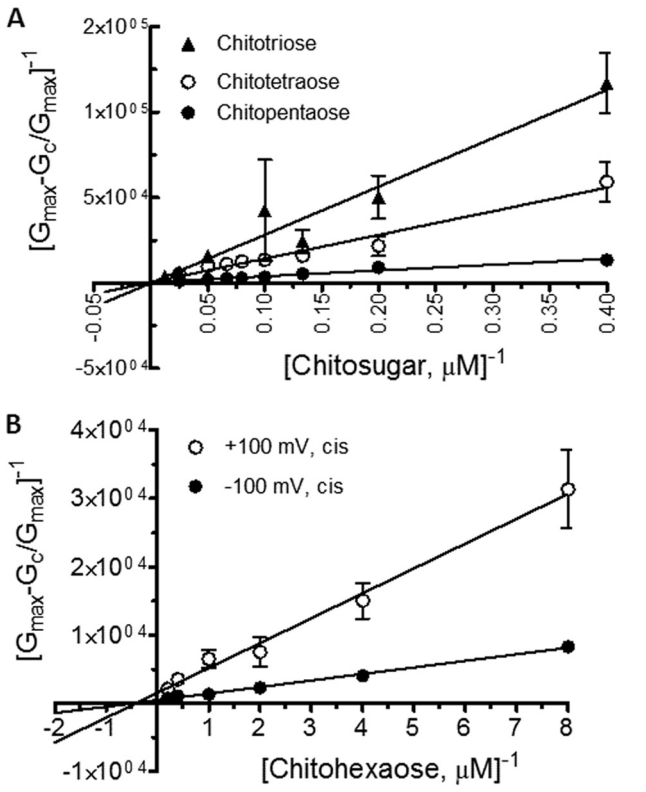

FIGURE 7. **Lineweaver-Burk plots for different chitosugars.** *A*, Lineweaver-Burk plots of chitotriose, chitotetraose, and chitopentaose at a concentration range of 2.5–40 μM. The conditions for data analysis were +100 mV/*cis*. *B*, Lineweaver-Burk plots of chitohexaose at +100 and −100 mV/*cis*. The equilibrium binding constant (*K*) can be obtained directly by fitting the curves with a linear regression function as described under "Results."

that, at 10 μM, chitotriose (Fig. 8*A*), chitotetraose (Fig. 8*B*), and chitopentaose (Fig. 8*C*) blocked only the *Vh*ChiP monomer. The second and third subunits were subsequently blocked when the sugar concentration was raised to 80 μM. The results suggest that *Vh*ChiP responded in a concentration-dependent manner not only toward chitohexaose but also toward lower molecular weight chitosugars. However, much higher concentrations of these sugars were required to induce multiple blockages due to their poor affinity as shown in Table 1.

The rate of sugar interaction (Fig. 4*A*) with *Vh*ChiP, the residence time within the channel (Fig. 4*C*), and its binding affinity (Table 1) were found to be highly dependent on the polarity of the applied potential. Voltage-dependent sugar permeation through the *Vh*ChiP pore likely reflected transient dipole moments due to the existence of the *N*-acetamido (–$NHCOCH_3$) groups of the multiple GlcNAc units that compose a chitooligosaccharide chain. As a result, the sugar chains seem to orient themselves favorably for channel entrance with a negative potential on the *cis* side and an opposite potential on the other side. The much higher rate of sugar permeation from *cis*-to-*trans* over *trans*-to-*cis* clearly indicates intrinsic asymmetry of channel. In the case of maltoporin, channel asymmetry was also observed; however, the effect was opposite that seen with *Vh*ChiP. The frequency of sugar diffusion into maltoporin from *trans*-to-*cis* was found to be significantly higher than from *cis*-to-*trans* (17–19). Such results indicate that the molecular arrangement contributing to

TABLE 1
Substrate specificity of *Vh*ChiP

Substrate	+100 mV/*cis*			−100 mV/*cis*		
	Binding constant (K)[a]	On-rate constant (k_{on})	Off-rate constant (k_{off})[b]	Binding constant (K)[a]	On-rate constant (k_{on})	Off-rate constant (k_{off})[b]
	M^{-1}	$10^6\ M^{-1}\ s^{-1}$	$10^3\ s^{-1}$	M^{-1}	$10^6\ M^{-1}\ s^{-1}$	$10^3\ s^{-1}$
Chitobiose	ND[c]			ND		
Chitotriose	220 ± 100	2.0 ± 0.2	9.0 ± 2.0	400 ± 150	5.0 ± 0.4	12.5 ± 2.5
Chitotetraose	2700 ± 700	10.0 ± 0.1	3.7 ± 0.11	5000 ± 850	15.2 ± 0.3	3.0 ± 0.40
Chitopentaose	15,000 ± 3000	25.5 ± 0.4	1.7 ± 0.13			
Chitohexaose	370,000 ± 140,000	78.0 ± 29.4	0.21 ± 0.02	500,000 ± 68,000	85.0 ± 1.4	0.17 ± 0.02

[a] The equilibrium binding constant (K) was determined by the titration method according to Equation 1.
[b] The on-rate constant (k_{on}) was estimated from $k_{on} = K \cdot k_{off}$. Because the residence time below 100 μs could not be evaluated with confidence, we therefore estimated the k_{on} of chitotriose from the number of blocking events/s. The resultant off-rate constant, in this case, was cross-calculated from $k_{off} = k_{on}/K$ instead.
[c] ND, no detectable blocking events with this sugar.

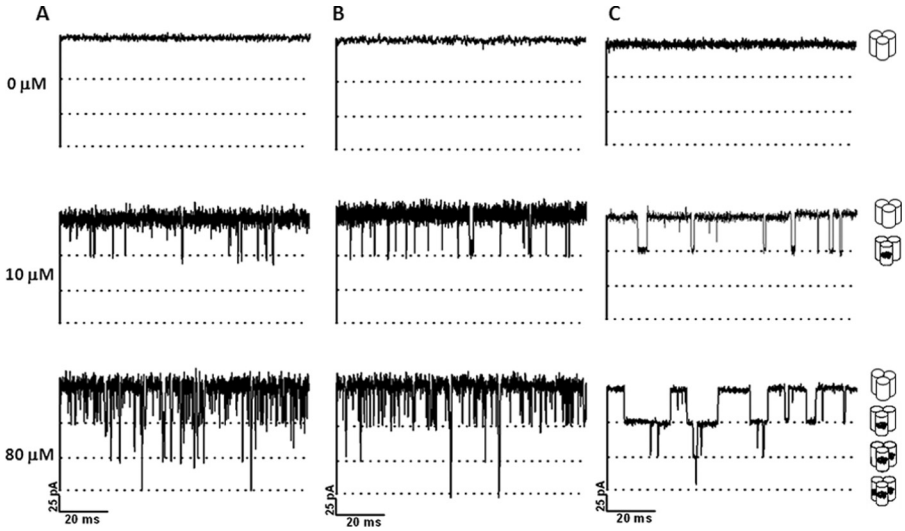

FIGURE 8. **Effects of concentrations of small chitosugars on ion current blockages.** A single channel of *Vh*ChiP was reconstituted into artificial lipid bilayers. Chitotriose (*A*), chitotetraose (*B*), and chitopentaose (*C*) were titrated on the *cis* side. Ion current blockages at +100 mV are presented.

TABLE 2
Comparison of the rates and the binding kinetics of *Vh*ChiP with those of other sugar-specific porins

Channel type	Substrate	K	k_{on}	k_{off}	Ref.
		M^{-1}	$10^6\ M^{-1}\ s^{-1}$	$10^3\ s^{-1}$	
*Vh*ChiP	Chitohexaose	500,000	85.0	0.17	This study
E. coli maltoporin (LamB)	Maltotriose	4300	8.4	1.95	Refs. 25, 33, 35, and 40
	Maltotetraose	8100	6.1	0.77	
	Maltopentaose	13,000	5.3	0.43	
	Maltohexaose	20,000	4.8	0.24	
	Maltoheptaose	31,000	5.6	0.18	
Salmonella typhimurium sucrose porin (ScrY)	Sucrose	80	0.004	0.05	Ref. 25
Klebsiella oxytoca cyclodextrin porin (CymA)	Cyclodextrin	31,300			Ref. 38
Pseudomonas putida glucose-inducible porin (OprB)	Glucose	9.1			Ref. 36
Pseudomonas aeruginosa glucose-inducible porin (OprB)	Glucose	2.6			Ref. 37

GlcNAc-binding subsite(s) within the *Vh*ChiP lumen is completely different from that in maltoporin.

Kinetic analysis indicated that *Vh*ChiP interacted with chitooligosaccharides in a concentration-dependent manner. However, there is a discrepancy regarding the size of the sugars. On-rates increased almost linearly for chitotriose and chitotetraose as their concentrations were increased. Diffusion through the *Vh*ChiP channel in these cases was driven entirely by the concentration gradient, with weak interactions between the sugar and protein molecules. However, the binding affinity significantly increased if the sugar chain was longer. Binding of chitopentaose to chitoporin was of particular interest because the sugar did not just transiently block the ion passage but appeared to interact strongly with the channel subunits at −100 mV/*cis*, yielding a permanent reduction of the channel conductance to one-third of the full conductance when its concentrations exceeded 50 nM (see Fig. 2*C* as a representative trace at 5 μM). As a result, we could not evaluate the binding constant of chitopentaose under this particular condition (Table 1). We do not yet completely understand why negative potentials strongly affect the permeation of chitopentaose. This will be a subject of our further investigation. Translocation of chitohexaose particularly involved specific substrate-protein interactions, resulting in Michaelis-Menten transport kinetics resembling those of previously reported sugar-specific porins, including maltoporin (LamB) (31–34), sucrose porin (ScrY) (25, 35), glucose-inducible porin (OprB) (36, 37), and cyclodextrin porin (CymA) (38, 39).

Our study revealed that chitohexaose is the most potent substrate of the *Vh*ChiP channel, as it blocked the ion flow even at nanomolar concentrations, and the monomeric subunit was already saturated below 1 μM. In Table 2, we summarize the rate constants: the on-rate (k_{on}) is by far the highest for chitohexaose, whereas the off-rate (k_{off}) is the lowest. Consequently, the resultant binding constant (K) of 5.0×10^6 M^{-1} is 1–5 orders stronger than the reported values for other analogs (25, 31, 35–40). According to the kinetic data in Table 2, *Vh*ChiP is the most active sugar-specific channel reported to date. A highly effective sugar transport machinery is considered to be crucial for *V. harveyi* to maintain the homeostatic balance that enables the bacterium to survive and thrive in extreme marine environments with a scarcity of the usual nutrients.

In conclusion, our quantification of the single channel turnover demonstrates the power of evolutionary pressure that drives marine bacteria (*V. harveyi* in our model study) to select for a highly active sugar-transporting system as a survival strategy in extreme aquatic environments. This mechanistic adaptation is not required by other bacteria that utilize glucose or sucrose as a common source of cellular energy.

Acknowledgment—We thank Dr. David Apps (Centre for Integrative Physiology, School of Biomedical Sciences, The University of Edinburgh, Edinburgh, United Kingdom) for critical proofreading of this manuscript.

REFERENCES

1. Austin, B., and Zhang, X. H. (2006) *Vibrio harveyi*: a significant pathogen of marine vertebrates and invertebrates. *Lett. Appl. Microbiol.* **43,** 119–124
2. Liuxy, P. C., Lee, K. K., and Chen, S. N. (1996) Pathogenicity of different isolates of *Vibrio harveyi* in tiger shrimp, *Penaeus monodon*. *Lett. Appl. Microbiol.* **22,** 413–416
3. Actis, L. A., Tolmasky, M. E., and Crosa, J. H. (2011) Vibriosis. in *Fish Diseases and Disorders: Viral, Bacterial and Fungal Infections* (Woo, P. T. K., and Bruno, D. W., eds) Vol. 3, 2nd Ed., pp. 570–605, CABI, Wallingford, United Kingdom
4. Li, X., and Roseman, S. (2004) The chitinolytic cascade in vibrios is regulated by chitin oligosaccharides and a two-component chitin catabolic sensor/kinase. *Proc. Natl. Acad. Sci. U.S.A.* **101,** 627–631
5. Jung, B. O., Roseman, S., and Park, J. K. (2008) The central concept for chitin catabolic cascade in marine bacterium, *Vibrio*. *Macromol. Res.* **16,** 1–15
6. Hunt, D. E., Gevers, D., Vahora, N. M., and Polz, M. F. (2008) Conservation of the chitin utilization pathway in the Vibrionaceae. *Appl. Environ. Microbiol.* **74,** 44–51
7. Bassler, B. L., Yu, C., Lee, Y. C., and Roseman, S. (1991) Chitin utilization by marine bacteria. Degradation and catabolism of chitin oligosaccharides by *Vibrio furnissii*. *J. Biol. Chem.* **266,** 24276–24286
8. Keyhani, N. O., Li, X. B., and Roseman, S. (2000) Chitin catabolism in the marine bacterium *Vibrio furnissii*. Identification and molecular cloning of a chitoporin. *J. Biol. Chem.* **275,** 33068–33076
9. Meibom, K. L., Li, X. B., Nielsen, A. T., Wu, C. Y., Roseman, S., and Schoolnik, G. K. (2004) The *Vibrio cholerae* chitin utilization program. *Proc. Natl. Acad. Sci. U.S.A.* **101,** 2524–2529
10. Yang, C., Rodionov, D. A., Li, X., Laikova, O. N., Gelfand, M. S., Zagnitko, O. P., Romine, M. F., Obraztsova, A. Y., Nealson, K. H., and Osterman, A. L. (2006) Comparative genomics and experimental characterization of *N*-acetylglucosamine utilization pathway of *Shewanella oneidensis*. *J. Biol. Chem.* **281,** 29872–29885
11. Suginta, W., Chumjan, W., Mahendran, K. R., Janning, P., Schulte, A., and Winterhalter, M. (2013) Molecular uptake of chitooligosaccharides through chitoporin from the marine bacterium *Vibrio harveyi*. *PLoS ONE* **8,** e55126
12. Prilipov, A., Phale, P. S., Van Gelder, P., Rosenbusch, J. P., and Koebnik, R. (1998) Coupling site-directed mutagenesis with high-level expression: large scale production of mutant porins from *E. coli*. *FEMS Microbiol. Lett.* **163,** 65–72
13. Garavito, R. M., and Rosenbusch, J. P. (1986) Isolation and crystallization of bacterial porin. *Methods Enzymol.* **125,** 309–328
14. Rosenbusch, J. P. (1974) Characterization of the major envelope protein from *Escherichia coli*. Regular arrangement on the peptidoglycan and unusual dodecyl sulfate binding. *J. Biol. Chem.* **249,** 8019–8029
15. Lugtenberg, B., and Van Alphen, L. (1983) Molecular architecture and functioning of the outer membrane of *Escherichia coli* and other gram-negative bacteria. *Biochim. Biophys. Acta* **737,** 51–115
16. Bezrukov, S. M., Kullman, L., and Winterhalter, M. (2000) Probing sugar translocation through maltoporin at the single channel level. *FEBS Lett.* **476,** 224–228
17. Schwarz, G., Danelon, C., and Winterhalter, M. (2003) On translocation through a membrane channel via an internal binding site: kinetics and voltage dependence. *Biophys. J.* **84,** 2990–2998
18. Danelon, C., Brando, T., and Winterhalter, M. (2003) Probing the orientation of reconstituted maltoporin channels at the single-protein level. *J. Biol. Chem.* **278,** 35542–35551
19. Kullman, L., Winterhalter, M., and Bezrukov, S. M. (2002) Transport of maltodextrins through maltoporin: a single-channel study. *Biophys. J.* **82,** 803–812
20. Mahendran, K. R., Chimerel, C., Mach, T., and Winterhalter, M. (2009) Antibiotic translocation through membrane channels: temperature-dependent ion current fluctuation for catching the fast events. *Eur. Biophys. J.* **38,** 1141–1145
21. Van Gelder, P., Dumas, F., and Winterhalter, M. (2000) Understanding the function of bacterial outer membrane channels by reconstitution into black lipid membranes. *Biophys. Chem.* **85,** 153–167
22. Winterhalter, M. (2000) Black lipid membranes. *Curr. Opin. Colloid Interface Sci.* **5,** 250–255
23. Berkane, E., Orlik, F., Charbit, A., Danelon, C., Fournier, D., Benz, R., and Winterhalter, M. (2005) Nanopores: maltoporin channel as a sensor for maltodextrin and lambda-phage. *J. Nanobiotech.* **3,** 3
24. Benz, R., and Hancock, R. E. (1987) Mechanism of ion transport through the anion-selective channel of the *Pseudomonas aeruginosa* outer membrane. *J. Gen. Physiol.* **89,** 275–295
25. Andersen, C., Cseh, R., Schülein, K., and Benz, R. (1998) Study of sugar binding to the sucrose-specific ScrY channel of enteric bacteria using current noise analysis. *J. Membr. Biol.* **164,** 263–274
26. Nikaido, H. (1992) Porins and specific channels of bacterial outer membranes. *Mol. Microbiol.* **6,** 435–442
27. Suginta, W., Robertson, P. A., Austin, B., Fry, S. C., and Fothergill-Gilmore, L. A. (2000) Chitinases from *Vibrio*: activity screening and purification of *chiA* from *Vibrio carchariae*. *J. Appl. Microbiol.* **89,** 76–84
28. Suginta, W. (2007) Identification of chitin binding proteins and characterization of two chitinase isoforms from *Vibrio alginolyticus* 283. *Enzyme Microb. Technol.* **41,** 212–220
29. Keyhani, N. O., and Roseman, S. (1999) Physiological aspects of chitin catabolism in marine bacteria. *Biochim. Biophys. Acta* **1473,** 108–122
30. Hjerde, E., Lorentzen, M. S., Holden, M. T., Seeger, K., Paulsen, S., Bason, N., Churcher, C., Harris, D., Norbertczak, H., Quail, M. A., Sanders, S., Thurston, S., Parkhill, J., Willassen, N. P., and Thomson, N. R. (2008) The genome sequence of the fish pathogen *Aliivibrio salmonicida* strain LFI1238 shows extensive evidence of gene decay. *BMC Genomics* **9,** 616
31. Andersen, C., Jordy, M., and Benz, R. (1995) Evaluation of the rate constants of sugar transport through maltoporin (LamB) of *E. coli* from the sugar-induced current noise. *J. Gen. Physiol.* **105,** 385–401
32. Benz, R., Schmid, A., Nakae, T., and Vos-Scheperkeuter, G. H. (1986) Pore formation by LamB of *Escherichia coli* in lipid bilayer membranes. *J. Bacteriol.* **165,** 978–986
33. Van Gelder, P., Dumas, F., Bartoldus, I., Saint, N., Prilipov, A., Winterhal-

ter, M., Wang, Y., Philippsen, A., Rosenbusch, J. P., and Schirmer, T. (2002) Sugar transport through maltoporin of *Escherichia coli*: role of the greasy slide. *J. Bacteriol.* **184,** 2994–2999
34. Klebba, P. E. (2002) Mechanism of maltodextrin transport through LamB. *Res. Microbiol.* **153,** 417–424
35. Van Gelder, P., Dutzler, R., Dumas, F., Koebnik, R., and Schirmer, T. (2001) Sucrose transport through maltoporin mutants of *Escherichia coli*. *Protein Eng.* **14,** 943–948
36. Saravolac, E. G., Taylor, N. F., Benz, R., and Hancock, R. E. (1991) Purification of glucose-inducible outer membrane protein OprB of *Pseudomonas putida* and reconstitution of glucose-specific pores. *J. Bacteriol.* **173,** 4970–4976
37. Wylie, J. L., Bernegger-Egli, C., O'Neil, J. D., and Worobec, E. A. (1993) Biophysical characterization of OprB, a glucose-inducible porin of *Pseudomonas aeruginosa*. *J. Bioenerg. Biomembr.* **25,** 547–556
38. Pajatsch, M., Andersen, C., Mathes, A., Böck, A., Benz, R., and Engelhardt, H. (1999) Properties of a cyclodextrin-specific, unusual porin from *Klebsiella oxytoca*. *J. Biol. Chem.* **274,** 25159–25166
39. Orlik, F., Andersen, C., Danelon, C., Winterhalter, M., Pajatsch, M., Böck, A., and Benz, R. (2003) CymA of *Klebsiella oxytoca* outer membrane: binding of cyclodextrins and study of the current noise of the open channel. *Biophys. J.* **85,** 876–885
40. Hilty, C., and Winterhalter, M. (2001) Facilitated substrate transport through membrane proteins. *Phys. Rev. Lett.* **86,** 5624–5627